Resonant tunneling of electromagnetic waves through polariton gaps

Lev I. Deych, D. Livdan, and A. A. Lisyansky
Department of Physics, Queens College, City University of New York, Flushing, New York 11367

(Received 25 November 1997)

We consider resonance tunneling of electromagnetic waves through an optical barrier formed by a stop band between lower and upper polariton branches. We show that the tunneling through this kind of barrier is qualitatively different from tunneling through other optical barriers as well as from the quantum-mechanical tunneling through a rectangular barrier. We find that the width of the resonance maximum of the transmission coefficient tends sharply to zero as the frequency approaches the lower boundary of the stop band. Resonance transmission peaks give rise to new photonic bands inside the polariton stop band in a periodic array of the barriers. [S1063-651X(98)13306-8]

PACS number(s): 42.25.Bs, 05.40.+j, 71.36.+c, 63.50.+x

I. INTRODUCTION

The effect of tunneling is well studied in the context of quantum mechanics (see, for example, Ref. [1]). Recently, tunneling of electromagnetic waves has attracted interest owing to experiments with evanescent electromagnetic waves [2–5], which are a direct analog of wave functions of tunneling quantum particles. These experiments provide an opportunity to experimentally study the time evolution of tunneling wave packets, a subject of long-standing controversy (see, for example, the review articles in [6–8]). So far, three types of optical barriers have been considered in the context of the tunneling experiments. Historically, the earliest an experiment with evanescent modes was carried out by Bose in 1927, where a prism with a beam incident at an angle larger than the angle of total internal reflection was used as a barrier [9]. The same idea was used by Yeh [10], who considered resonant tunneling of electromagnetic waves in a superlattice composed of alternating layers with indices of refraction such that the incident angle was greater than the angle of total internal reflection for one layer and smaller for the other one. The majority of time-of-flight theoretical considerations and experiments have been performed for an undersized waveguide [4,2,11] and photonic band gaps [3,5]. All of the considered optical barriers were artificial structures. However, there exist natural optical barriers, which are well known, but were never considered in the context of light tunneling. We are referring to ''restrahlen'' or ''stop'' photonic bands, which exist in many dielectrics and semiconductors in the region of polariton resonances. It is well known that in the absence of attenuation, the transmission coefficient of light with a frequency within the stop band decreases exponentially with an increase in the width of a slab through which it propagates. Therefore, a simple slab of a dielectric with polariton resonances can serve as a ''naturally made'' photonic barrier. Properties of this polariton barrier, however, might be considerably different from properties of other kinds of barriers because of the different dispersion law of electromagnetic waves tunneling through the polariton barrier. It is important, therefore, to consider the tunneling properties of polariton barriers.

In this paper we consider tunneling of electromagnetic radiation through a polariton barrier in a steady-state mode. The point of interest in this situation is the resonance tunneling through a two-barrier system. Resonance tunneling of electromagnetic waves in a superlattice structure was previously discussed in Ref. [10]. A tunneling effect in Ref. [10] arose when the angle of incidence for electromagnetic waves exceeded the angle of total internal reflection for one of the layers constituting the superlattice. The frequency dependence of the imaginary wave number in this case coincides with that of the square-barrier quantum tunneling problem. The situation considered in this paper is considerably different. The imaginary wave number in a polariton barrier layer depends upon the frequency in a peculiar way, demonstrating a singularity near the lower boundary ω_T of the polariton gap. This dependence does not have an analog in quantum-mechanical systems. This leads to a different pattern of resonance tunneling states.

Extending our system from two barriers to a periodic array of alternating transparent and barrier layers, we obtain photon bands *inside the initial forbidden band*. These bands arise from the tunneling states and inherit many of their properties. In particular, we show that the bandwidths of these bands are determined by the widths of the respective resonances. The band structure of two- and three-dimensional photonic crystals made of materials with frequency-dependent dielectric permeability was numerically studied in Refs. [12–14]. Maradudin and McGurn [12,13] computed bands of two- and three-dimensional structures composed of metal rods (spheres in the three-dimensional case) with dielectric permeability of the form $\varepsilon=1-\omega_p^2/\omega^2$, where ω_p is the frequency of plasma excitations in the metal. Zhang *et al.* [14] dealt with a photonic crystal built of a dielectric with ε similar to that used in the present paper [see Eq. (1) below]. One of the interesting effects observed in both studies was flattening of the photonic bands below the frequency ω_p, in the case considered in Ref. [12], or below ω_T for Ref. [14]. We show analytically that this effect in the case of the dielectric photonic crystal is a direct consequence of the singular behavior of the dielectric function at ω_T. We also discuss the influence of absorption upon tunneling properties of the polariton barriers.

II. RESONANCE TUNNELING IN A THREE-LAYER SYSTEM

We consider propagation of electromagnetic radiation of frequency ω in a system that consists of two parallel absorbing dielectric layers, each of thickness a, positioned along the x axis and separated by a distance b. The dielectric permeability of the dielectric material is given by

$$\varepsilon(\omega)=\varepsilon_\infty \frac{(\omega+i\gamma)^2-\omega_L^2}{(\omega+i\gamma)^2-\omega_T^2}, \tag{1}$$

where γ is the attenuation and ε_∞ is the background dielectric permeability. Both layers are considered optically isotropic, so that TE and TM waves are not coupled. This allows us to neglect the vector nature of the electric field. We consider the case of normal incidence so that the electric field in our system can be presented as

$$E(x)=\begin{cases} e^{ik_0x}+re^{-ik_0x}, & 0\geqslant x>-\infty \\ a_1e^{ikx}+b_1e^{-ikx}, & a\geqslant x>0 \\ a_2e^{ik_0(x-a)}+b_2e^{-ik_0(x-a)}, & a+b\geqslant x>a \\ a_3e^{ik(x-a-b)}+b_3e^{-ik(x-a-b)}, & 2a+b\geqslant x>a+b \\ te^{ik_0(x-2a-b)}, & x>2a+b, \end{cases} \tag{2}$$

where $k_0=\omega/c$ is the wave vector in vacuum, c is the speed of light in vacuum, and r, a_1, b_1, a_2, b_2, a_3, b_3, and t are the complex amplitudes of the plane waves in each of the five different regions. The wave number k in the dielectric layers is determined by the expression following from Eq. (1):

$$k=k_0\sqrt{\varepsilon_\infty \frac{(\omega+i\gamma)^2-\omega_L^2}{(\omega+i\gamma)^2-\omega_T^2}}. \tag{3}$$

Taking into account regular boundary conditions at each of the boundaries between different materials, we obtain the following expression for the complex transmission coefficient t:

$$t=16\left(\frac{k}{k_0}\right)^2 e^{2ika+ik_0b}\left(1-\frac{k^2}{k_0^2}\right)^{-2}\Bigg[2e^{2ika+ik_0b}-2e^{2ika} -e^{ik_0b}-e^{4ika+ik_0b}+\left(1-4\frac{k}{k_0}+6\frac{k^2}{k_0^2}-4\frac{k^3}{k_0^3}+\frac{k^4}{k_0^4}\right)e^{4ika} +1+4\frac{k}{k_0}+6\frac{k^2}{k_0^2}+4\frac{k^3}{k_0^3}+\frac{k^4}{k_0^4}\Bigg]^{-1}. \tag{4}$$

In the case of a lossless dielectric ($\gamma=0$) the expression for the transmissivity of the system $T=|t^2|$ can be obtained as

$$T=\frac{1}{1+\left(\dfrac{\kappa}{k_0}+\dfrac{k_0}{\kappa}\right)^2\sinh^2(\kappa a)\cos^2[K(a+b)]}, \tag{5}$$

where $K(a+b)$ is given by

$$\cos[K(a+b)]=\cosh(\kappa a)\cos(k_0b)+\frac{1}{2}\left(\frac{\kappa}{k_0}-\frac{k_0}{\kappa}\right)\sinh(\kappa a)\sin(k_0b). \tag{6}$$

We assume here that the frequency of the wave falls into the region $\omega_T<\omega<\omega_L$ so that the wave number $k=i\kappa$ is imaginary and propagation of the wave through the dielectric layers is evanescent. Equation (5) describes optical tunneling through a forbidden ''band.'' However, for a set of frequencies such that

$$\cos[K(a+b)]=0, \tag{7}$$

the transmission coefficient T is equal to 1 and tunneling through the system becomes resonant. Though Eq. (6) is similar to the respective equations of Ref. [10] and of the quantum-mechanical tunneling problem, the different frequency dependence of the wave number k causes different behavior of the solutions to this equation.

In order to determine the number of resonance frequencies, it is convenient to rewrite Eq. (7) as

$$\frac{1}{2}\left(\frac{k_0}{\kappa}-\frac{\kappa}{k_0}\right)\tanh(\kappa a)=\cot(k_0b). \tag{8}$$

If boundary frequencies ω_L and ω_T satisfy the inequality

$$\omega_L-\omega_T<\frac{\pi c}{b}, \tag{9}$$

the respective interval of wave numbers form ω_T/c to ω_L/c can only accommodate less than one period of cot(k_0b). In this case Eq. (8) has one solution if

$$k_0a\tan(k_0b)>2. \tag{10}$$

If inequality (9) does not hold, the number of resonance frequencies is equal to

$$N=\frac{(\omega_L-\omega_T)b}{\pi c}+1 \tag{11}$$

if inequality (10) is satisfied and it is $N-1$ otherwise. The transmission T as a function of frequency is presented in Fig. 1 for two different values of the widths of the layers a and b. One can see that as the ratio of a to b increases, so does the number of resonant peaks.

Both plots in Fig. 1 show a similar pattern: the separation between resonant peaks remains approximately constant while the half-width Γ of peaks sharply decreases as the frequency approaches ω_T. The resonant half-width Γ can be found by expanding the denominator of Eq. (5) near the resonance frequency ω_r up to the term quadratic in $\omega-\omega_r$. If a resonance frequency ω_r is close to the lower boundary of the gap ω_T, one can find for Γ

$$\Gamma\approx\frac{2\sqrt{2}}{k_0a}\frac{(\delta\omega)^2}{\omega_*}\exp\left[-2(k_0a)\left(\frac{\omega_*}{\delta\omega}\right)^{1/2}\right], \tag{12}$$

where $\delta\omega=\omega_T-\omega_r$ and $\omega_*=\epsilon(\omega_L^2-\omega_T^2)/2\omega_T$. Equation (12) describes an extremely sharp nonanalytical behavior of

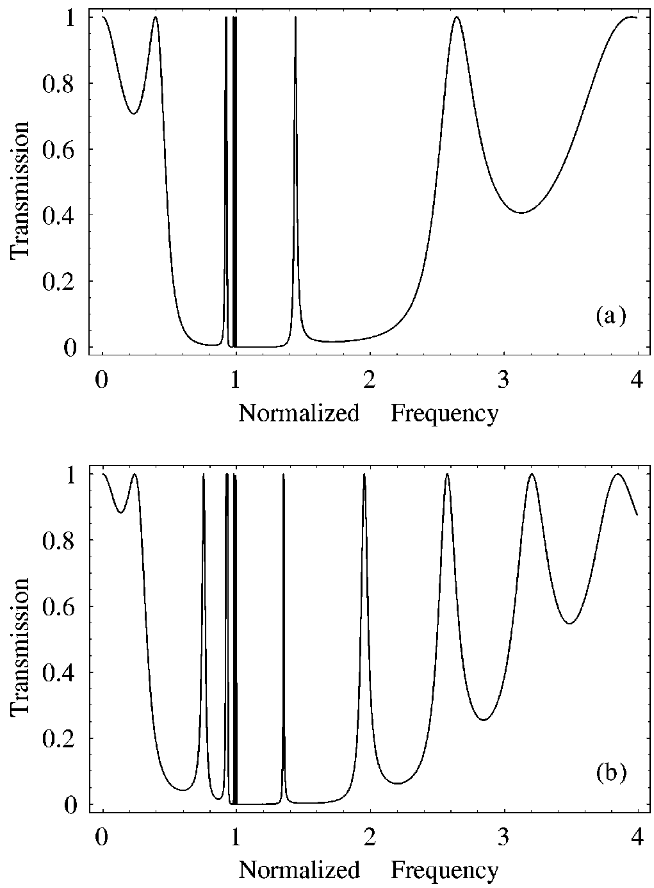

FIG. 1. Transmission as a function of ω/ω_T. The ratio of ω_L/ω_T is equal to 3 for both plots. (a) Values of a and b are 2 and 8, respectively. (b) $a=2$ and $b=20$. The polariton gap lies between normalized frequencies 1 and 3.

the width of the resonance near the low-frequency boundary of the gap. To take absorption into account, one can replace the parameter $\delta\omega$ by the expression

$$\delta\omega_{abs}=\sqrt{(\omega_T-\omega_r)^2+\gamma^2}.$$

If $\omega_T-\omega_r<\gamma$ the width of the resonance becomes proportional to $\exp(-\omega_*/\gamma)^{1/2}$ and remains small for $\gamma<\omega_*$. However, the width grows exponentially fast with an increase of the absorption rate and the height of the peak decreases correspondingly. Therefore, the resonances nearest ω_T are the most vulnerable with respect to absorption. One can see this in Fig. 2, which shows that these resonances disappear first when the absorption becomes larger. It also follows from this analysis that the width of the resonance peaks close to ω_T is determined solely by absorption. This behavior of the resonances is specific to our particular model and does not take place in the case of Ref. [10], where the wave vector is finite for any ω in the forbidden band.

When ω_r approaches ω_L, the wave vector $\kappa(\omega_r)$ becomes smaller and Γ increases with frequency, reaching at $\omega_0\simeq\omega_L$ a certain value, which depends upon all the parameters of the system. For these frequencies, absorption, when small enough, does not contribute significantly to the width of the maxima.

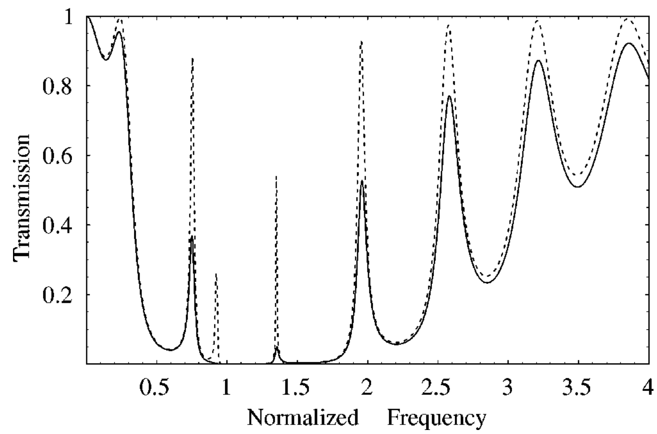

FIG. 2. Transmission in the presence of absorption for $a=2$ and $b=8$. The dashed line corresponds to an attenuation coefficient $\gamma/\omega_T=0.005$ and the solid line depicts the transmission for $\gamma/\omega_T=0.05$.

III. PHOTONIC BANDS IN THE POLARITON FORBIDDEN GAP

In the case of a periodic array of the three-layer sandwiches considered in the preceding section, one has a set of propagating bands instead of single resonance frequencies. In this situation, Eq. (6) presents the dispersion equation of the propagating modes with K being the Bloch wave number. The resonant tunneling frequencies discussed in the preceding section are the solutions of the dispersion equation at the center of the Brillouin band, $K(a+b)=\pi/2$, where $K(a+b)$ changes between 0 and π within the band. It is clear, therefore, that each of the resonances gives rise to a corresponding band. This conclusion is supported by the dispersion curves plotted in Fig. 3. One can see from this figure that for each resonant frequency ω_{rn}, where n is the number of a given mode, there is a distinct branch of the dispersion curve. It is interesting to note that branches corresponding to the resonant frequencies close to ω_T have much smaller dispersion than branches that correspond to $\omega_r\simeq\omega_L$. One can also notice that regular bands, which appear outside the polariton gap, also become less dispersive for frequencies near ω_T. This observation agrees with the results reported in Refs. [12–14] for two-dimensional systems. The advantage of the one-dimensional model is that we can analytically determine the cause for this behavior. Assuming that the width of a band, centered at ω_{rn}, is much smaller than the frequency itself, one can expand the right-hand side of the dispersion equation (6) with respect to $\omega-\omega_{rn}$ and obtain the approximate dispersion equation as

$$\omega-\omega_{rn}=(-1)^n\Gamma(\omega_{0n})\left(\frac{\kappa}{k_0}+\frac{k_0}{\kappa}\right)\sinh[\kappa(\omega_{0n})a]\times\cos[K(a+b)]. \tag{13}$$

If one combines this equation and Eq. (12) for the resonance width Γ, the expression for the bandwidth, $\Delta\omega_n$ for bands near the lower edge ω_T becomes

$$\Delta\omega_n\sim\frac{(\delta\omega)^2}{\omega_*}.$$

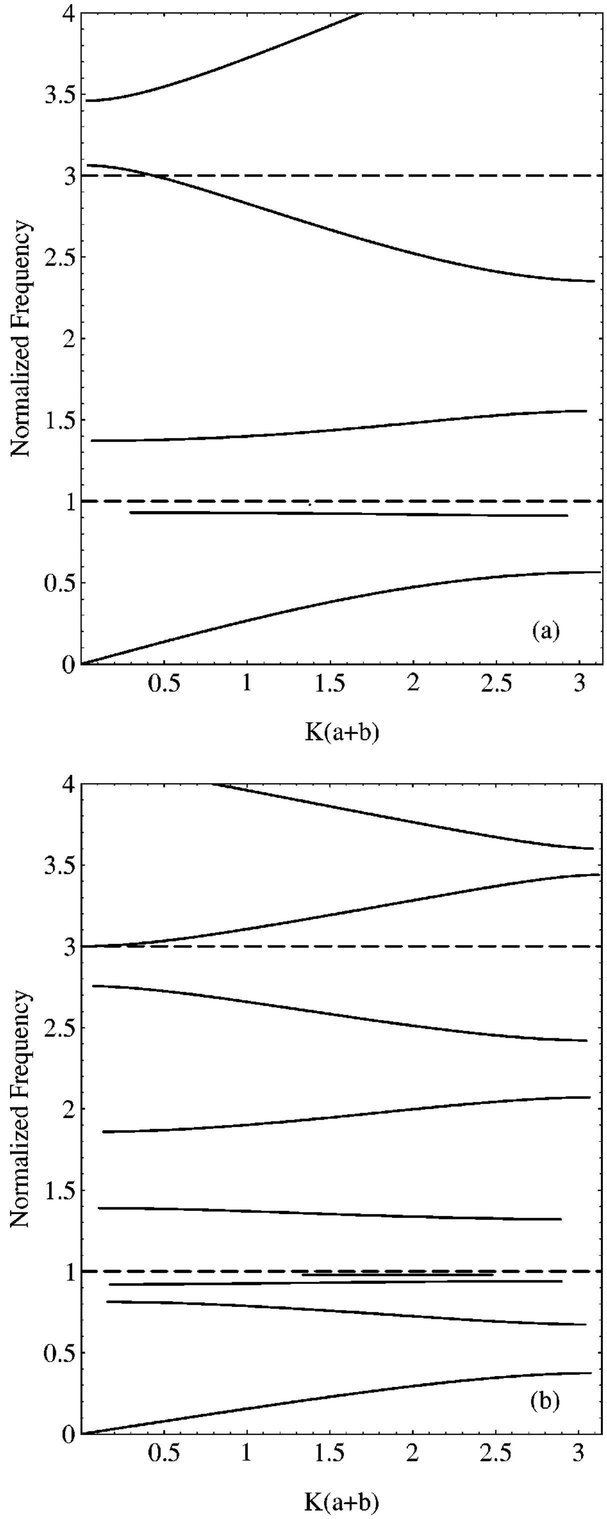

FIG. 3. Bands arising in the polariton gap in the case of periodic arrangement of the considered system. (a) $a=2$, $b=8$ and (b) $a=2$, $b=20$. The polariton gap is shown by dashed lines. Dispersion curves in the forbidden gap correspond to the resonant peaks from Fig. 1.

This expression also holds for frequencies at the pass-band side of ω_T and explains, therefore, the flattening of the photon dispersion curves near ω_T observed in Refs. [12–14]. Both the bandwidth $\Delta\omega_n$ and the width of the resonance Γ tend to a certain finite value when ω approaches ω_L. The prefactor $(-1)^n$ in Eq. (13) shows that the branches have an alternating sign of the dispersion: positive for the ''even'' branches and negative for the ''odd'' ones. This feature is clearly seen in Fig. 3.

IV. CONCLUSION

We consider a polariton stop band (restrahlen region) as an optical barrier for tunneling of electromagnetic waves. We show that the peculiar frequency dependence of the tunneling penetration length of electromagnetic waves results in tunneling properties that are qualitatively different from those of other optical barriers. We carry out a detailed study of the resonant tunneling of electromagnetic waves through a three-layer sandwich, where a dispersionless (vacuum) layer was placed between two identical layers with dielectric permeability allowing for the polariton stop band. It was found that the number of resonance frequencies depends upon the frequency width of the stop band $\omega_L-\omega_T$ and the spatial width b of the vacuum layer. This number increases with an increase of $\omega_L-\omega_T$ and b. The latter dependence appears paradoxical since it implies that no matter how far away tunneling layers are from each other, they are capable of providing conditions for resonant tunneling. The situation becomes clear if one recollects that we deal with the steady-state situation, where the flux of energy in the system is fixed by an external source. For a large system, a wave has to travel a long distance between the layers before it reaches the steady-state condition. This fact is crucial for an experimental observation of resonance tunneling since one has to have a steady enough source of light and be able to maintain a complete coherence of the wave while it travels between the layers. Let us consider, for example, GaAs, for which $\omega_T=5.1\times10^{13}$ s^{-1} and $\omega_L=5.5\times10^{13}$ s^{-1} [15]. The vacuum wavelength in this case changes between 34 and 37 μm when the frequency sweeps over the polariton gap. If one makes the distance b between the layers equal to, say, 350 μm (approximately ten wavelengths), then the number of observable resonances would be equal to 1 or 2 depending upon the width of the dielectric layers. In order to observe a greater number of the resonance one could use materials with wider polariton gaps, for example, MgO, where $\omega_T=7.5\times10^{13}$ s^{-1} and $\omega_L=14\times10^{13}$ s^{-1} [15]. In this case even for b as small as 60 μm , four resonance peaks could be observed. The actual number of resonance maxima also depends upon relaxation characteristics of the layers. Though these characteristics can vary even for different samples of the same type of material, one can consider $\gamma=0.02$ [16] as a typical value and use it for quantitative estimates. It is seen from Fig. 2 that the relaxation of this order of magnitude could reduce the number of observable resonances by at most one maximum if the configuration of the system allows for a maximum near ω_T. More specific conclusions regarding the number of the expected resonances could be drawn from the results of the paper for each particular experimental configuration.

The width of the resonance peaks of the transmission coefficient was found to have a sharp nonanalytical frequency dependence at the lower boundary of the polariton gap ω_T and to saturate at a certain finite value when approaching the upper boundary ω_L. This results in different reactions to absorption for resonances occurring in the vicinities of ω_T and ω_L. In the first situation even a small absorption completely determines the real width of the resonance and these resonances are eliminated first with an increase of absorption. The resonances in the latter case survive a much stronger rate of absorption and for a small one they have a width mainly determined by the properties of the barrier itself.

We also consider the extension of our system to a periodic array of the sandwiches. We show that each of the resonances of the original system gives rise to a band, with the original resonance frequency at the center of the respective band. The bandwidths of the bands (and correspondingly their degrees of dispersion) are found to be determined by the frequency width of the respective parent resonances. This explains flattening photonic bands near ω_T observed previously in numerical simulations of two-dimensional systems [14].

ACKNOWLEDGMENTS

We wish to thank S.A. Schwarz for reading and commenting on the manuscript. This work was supported by the NSF under Grant No. DMR-9632789, by a CUNY collaborative grant, and by PSC-CUNY.

[1] D.K. Roy, *Quantum Mechanical Tunneling and its Applications* (World Scientific, Singapore, 1986).
[2] A. Enders and G. Nimtz, J. Phys. I **2**, 1693 (1992); **3**, 1089 (1993); Phys. Rev. B **47**, 9605 (1993); Phys. Rev. E **48**, 632 (1993).
[3] A.M. Steinberg, P.G. Kwiat, and R.Y. Chiao, Phys. Rev. Lett. **71**, 708 (1993).
[4] A. Ranfagni, D. Mugnai, P. Fabeni, and G.P. Pazzi, Appl. Phys. Lett. **58**, 774 (1991); A. Ranfagni, P. Fabeni, G.P. Pazzi, and D. Mugnai, Phys. Rev. E **48**, 1453 (1994).
[5] Ch. Spielmann, R. Szipocs, A. Stingl, and F. Krausz, Phys. Rev. Lett. **73**, 2308 (1994).
[6] R. Landauer and Th. Martin, Rev. Mod. Phys. **66**, 217 (1994).
[7] E.H. Hauge and J.A. Stovneng, Rev. Mod. Phys. **61**, 917 (1989).
[8] V.S. Olkhovsky and E. Recami, Phys. Rep. **214**, 329 (1992).
[9] J. Ch. Bose, Bose Institute Transaction **1927**, 42.
[10] P. Yeh, J. Opt. Soc. Am. A **2**, 568 (1985).
[11] Th. Martin and R. Landauer, Phys. Rev. A **45**, 2611 (1992).
[12] A.A. Maradudin and A.R. McGurn, J. Opt. Soc. Am. B **10**, 307 (1993).
[13] A.R. McGurn and A.A. Maradudin, Phys. Rev. B **48**, 17 576 (1993).
[14] W. Zhang, A. Hu, X. Lei, N. Xu, and N. Ming, Phys. Rev. B **54**, 10 280 (1996).
[15] C. Kittel, *Introduction to Solid State Physics* (Wiley, New York, 1986).
[16] *Handbook of Optical Constants of Solids*, edited by Edward D. Palik (Academic, New York, 1991).